Title

Depth profile of uncompensated spins in an exchange bias system

Authors

Roy, S.
Fitzsimmons, M.R.
Park, S.
et al.

Publication Date

2005-05-17

Depth profile of uncompensated spins in an exchange bias system

S. Roy,[a] M.R. Fitzsimmons,[b] S. Park,[b] M. Dorn,[a] O. Petracic,[a,c] Igor V. Roshchin,[a] Zhi-Pan Li,[a] X. Batlle,[a,d] R. Morales,[a,e] A. Misra,[b] X. Zhang,[b] K. Chesnel,[f] J.B. Kortright,[f] S.K. Sinha[a,b] and Ivan K. Schuller[a]

[a]*Department of Physics, University of California at San Diego, La Jolla, CA 92093 USA*

[b]*Los Alamos National Laboratory, Los Alamos, NM 87545 USA*

[c]*Angewandte Physik, Universität Duisburg-Essen, 47048 Duisburg, Germany*

[d]*Departament de Fisica Fonamental, Universitat de Barcelona, 08028 Barcelona, Catalonia, Spain*

[e]*Departamento de Fisica, Universidad de Oviedo, c/ Calvo Sotel s/n, Oviedo 33007, Spain*

[f]*Lawrence Berkeley National Laboratory, Berkeley, CA 94720 USA*

The spin structure of an antiferromagnet plays a critically important role in magnetic devices; however, the spin structure at the surface and interior of an antiferromagnetic thin film remains unknown. Here, we have used the unique spatial sensitivity of polarized neutron and soft X-ray beams in reflection geometry to measure the depth dependence of magnetization across the interface between a ferromagnet and an antiferromagnet. The net uncompensated magnetization near the interface responds to applied field, while uncompensated spins in the antiferromagnet bulk are pinned; thus, providing a means to establish a magnetic reference state.

PACS numbers: 75.70.Ak, 75.70.Cn, 61.12.-q, 61.10.-i

Development of magnetic devices, such as spin valves found in magnetic recording heads or magnetic random access memory, involves understanding the influence of physical confinement of materials (at the nanometer length scale) on magnetic phenomena.[1] An example is exchange bias,[2,3,4,5,6] which is observed as a shift of the ferromagnetic hysteresis loop along the field axis, observed in ferromagnetic-antiferromagnet (F-AF) systems. The shift is attributed to the exchange coupling between the F and AF across the interface. Exchange bias serves as a means to establish a magnetic reference in a spin valve.

The dependence of exchange bias[2,3] on environmental variables such as field,[7,8,9] temperature[10] and strain[11] is commonly attributed to changes in the AF domain state,[12] or the metastability of the spin structure in the AF film bulk or at the F-AF interface.[13] Indeed, a neutron scattering study of exchange biased Co/$LaFeO_3$ [14] and an X-ray magnetic circular dichroism study of exchange biased Co/$Ir_{0.8}Mn_{0.2}$ [15] each observed a correlation between exchange bias and pinned magnetization in the antiferromagnet. Yet, detailed information about the depth dependence of the spin structures of AF domains, particularly at the F-AF interface and extending into the AF film bulk is mostly lacking for exchange bias systems. There is a compelling need to know the distribution of uncompensated magnetization at the F-AF interface and in the AF bulk when in proximity to a ferromagnet, and the response of uncompensated magnetization to magnetic field.

We have used polarized neutron and soft X-ray beams in reflection geometry to measure the depth profile of magnetization across the F-AF interface and inside the AF film with unprecedented sensitivity. Measurement with neutron beams provides the variation of the *vector* magnetization (in our case its projection onto the sample plane)[16] in absolute units, and measurement with circularly polarized X-ray beams tuned to the *L*-edges of the magnetic atoms provides the variation of the element specific magnetization projected onto the incident beam axis.[17,18,19] For a Co/FeF_2 bilayer—an often studied model exchange biased system—we find that the net uncompensated magnetization in the FeF_2 antiferromagnet as far as 3.5 nm from the Co/FeF_2 interface responds to applied field, and this magnetization is anti-parallel to the Co magnetization. In the remainder of the FeF_2 layer, the uncompensated magnetization is pinned. Our observations motivate an alternative explanation of exchange bias that attributes bias to spins that are pinned in the antiferromagnet bulk, rather than at the F-AF interface.

Exchange bias samples were prepared by sequential electron beam evaporation of FeF_2, Co and Al at a deposition rate of 0.05 nm/s onto (110) oriented single crystal MgF_2 polished substrates measuring 10 mm by 10 mm. The deposition temperatures were 300 °C for the FeF_2 layer and 150 °C for the Co and Al layers. The chemical structure of the sample was determined from an analysis of the sample's reflectivity acquired with non-resonant X-rays and was not subject to refinement in subsequent analyses of the resonant soft X-ray or neutron data. The thickness of the Co (FeF_2) layer was 4.1±0.1 nm (36.6±0.1 nm), and the structural roughness of the Co/FeF_2 (FeF_2/MgF_2) interface was 0.5±0.1 nm (0.4±0.1 nm). A comparison of the off-specular X-ray reflectivity to the specular X-ray reflectivity[20] indicates that the roughnesses of the two interfaces were uncorrelated.

In-plane glancing angle X-ray diffraction and transmission electron microscopy confirmed that the AF layer was an untwinned single crystal film with $[1\bar{1}0]$ FeF_2 || $[1\bar{1}0]$ MgF_2, and surface normal along [110] FeF_2.[21] The ~1.8° widths of in-plane Bragg reflections from the FeF_2 single crystal were about four times broader than the reflections from the MgF_2 substrate. The dislocation density[22] at the FeF_2/MgF_2 interface corresponds to an average spacing between dislocations of ~55 nm; however, were all the misfit strain in the FeF_2 film relieved, we would expect the spacing to be 21 nm.[23] Therefore, only a fraction of the total misfit strain relieved is relieved in the FeF_2 film. Defects and strain (through piezomagnetism) can produce uncompensated magnetization in an antiferromagnet such as FeF_2.[11]

The resonant soft X-ray scattering experiment was performed using a circularly polarized incident X-ray beam (geometry shown in the inset of Figure 1). The sample was cooled to 20 K in a field of H_{FC} = 796 kA/m (cooling field) applied along [001] FeF_2 (to establish bias). The sample and detector were rotated about $[\bar{1}10]$ FeF_2. The intensity of the specularly reflected radiation was recorded as a function of incident beam polarization, applied field $\vec{H}$, and wavevector transfer Q (= $k_f - k_i$,, see Figure 1). The incident X-ray wavelength was tuned to either the Co-L_3 or Fe-L_3 edge such that the signs of the charge and magnetic scattering factors were the same. In the first measurement, we held the angles of incidence and reflection fixed at 3° (relative to the sample surface), and recorded the reflected intensity for left and right circularly polarized light, I_{P+} and I_{P-} (polarization = ±90%) as a function of H. Magnetization loops (Figure 1) corresponding to Co (■, Q = 0.49 nm^{-1}) or Fe (●, Q = 0.38 nm^{-1}) spins[24] exhibit hysteresis indicating that some Co and Fe spins are unpinned. Both loops are shifted along the positive field axis (also parallel to H_{FC}) by the bias field, H_E = +167±4 kA/m. Since the coercivity and bias obtained from either loop are the same, the Co and Fe spins are likely coupled. Along the magnetization axis, the curves are inverted—indicating that the Co and Fe spins are anti-parallel (for this Q).[25]

We performed a second soft X-ray experiment that involved measuring the reflected beam intensity as a function of Q, for one incident X-ray beam polarization for H = ±796 kA/m. This protocol is sensitive to changes in the specular reflectivity due to the reversal of unpinned spins. From the variation of I_{H+} and I_{H-} with Q (Figure 2, inset)—here, the subscript refers to H being parallel (+) or anti-parallel (-) to H_{FC}—the depth profiles of the Co and Fe spins can be obtained for each field direction. A theory for reflectometry with resonant X-ray beams based on a generalization of the Distorted Wave Born Approximation was used to analyze the data.” We chose to treat the Co magnetization as rotatable, but retained the possibility for having both unpinned Fe spins and Fe spins pinned along the direction of the cooling field. Using this model, the reflectivities for the two directions of H were calculated from the spin density profile shown in Figure 2 to obtain the solid curves (inset) which are those yielding a minimum χ^2 (best fit).[26] The spin profile represents the projection of the net magnetization of Co or Fe along the incident beam axis, which is nearly parallel to $\vec{H}$.[27] We see a change of the Fe spin magnetization from negative to positive values over a distance of ~2 nm *below* the Co/FeF_2 interface. The changes in the projections of the Co and Fe spins along $\vec{H}$ with depth occur over a distance much larger than that corresponding to interdiffusion or chemical roughness across the Co/FeF_2 interface, which could be explained by the presence of magnetic domains at the interface, or the rotation of magnetization away from the field axis.

We undertook a polarized neutron reflectometry [28,29] study of the sample including polarization analysis in order to determine whether the spatial variation of the net magnetization vector[30] in the Co and FeF_2 layers could be attributed to a domain wall parallel to the Co/FeF_2, and to obtain the depth profile of the pinned magnetization. After cooling the sample in a 438 kA/m field along [001] FeF_2 to 10 K (to establish bias), we rotated the sample about its surface normal in this field, so that $\vec{H}$ was parallel to $[\bar{1}10]$ FeF_2 (Figure 3 inset). The intent of applying $\vec{H}$ during the neutron measurement in a direction different than the cooling field (with a strength exceeding the anisotropy field of the sample) was to perturb the magnetization so that we could determine where the magnetization was pinned (in the direction of the cooling field) or unpinned. The polarized neutron reflectivity of the sample is shown in Figure 3, after removal of instrumental background and correction for polarization efficiencies. The large difference between the two non-spin-flip *(NSF)* reflectivities (corresponding to the intensities measured for fixed incident and reflected neutron polarization, either both spin-up R^{++}, or both spin-down R^{--}) is related to the component $M_{||}$ of the net magnetization vector that follows $\vec{H}$ and lies in the sample plane. The spin-flip *(SF)* reflectivity R^{SF} (the average of the intensities of the neutron beam whose polarization is flipped from spin-up to down, and vice versa), [Figure 3 (green symbols)] is related to the component $M_{\perp}$ of the net magnetization vector that is perpendicular to $\vec{H}$ and lies in the sample plane. From measurements of R^{NSF} and R^{SF}, the depth profile of the net magnetization vector projected onto the sample plane can be obtained quantitatively. Even in the absence of quantitative fitting (discussed later), the observation of non-zero *SF* reflectivity in Figure 3 means that the field of 438 kA/m applied during the neutron measurement perpendicular to the cooling field axis [001], was not sufficient to rotate the entire sample magnetization parallel to the applied field. We regard the portion of the magnetization that does not respond to field as pinned in the [001] direction, since the field during the measurement was applied along the $[\bar{1}10]$ direction—a direction that was perpendicular to the cooling field.

We note that *SF* reflectivity was not observed when the field during the neutron measurement was applied parallel to the cooling field. Nor, was *SF* reflectivity observed when the measurement field was applied perpendicular to the cooling field *and* the temperature of the sample was 108 K—significantly above the ordering temperature T_N = 78 K of FeF_2.

Quantitative information about the locations of unpinned and pinned uncompensated magnetization in the sample was obtained from an analysis of the Q dependence of the neutron reflectivity using the Parratt formalism.[31] The magnetic structure of the model was divided into three regions representing magnetization in the Co layer (with magnitude M_{Co} [32] and direction ϕ_{Co}, in the sample plane relative to the applied field), the interface (M_{int}, ϕ_{int}), and the FeF_2 bulk (M_{FeF2}, ϕ_{FeF2}). The magnetization of one region was connected to the next using an error function with width σ (each magnetic interface had an adjustable width).[33] The magnetic thickness of the interface was adjusted at the expense of the FeF_2 magnetic layer thickness. The model contains eight adjustable parameters, and these parameters were optimized to obtain the depth profiles shown in Figure 4 from which R^{++}, R^{--}, and R^{SF} (solid curves, Figure 3) are obtained.

The magnetization in the Co film is mostly parallel to $\vec{H}$ except near the Co/FeF_2 interface where the magnetization rotates in the positive sense away from the applied field by ϕ_{Co} = +16° (red curve, Figure 4), against the cooling field. The uncompensated magnetization in the FeF_2 rotates in the opposite sense to be ϕ_{int} = -30° near the Co/FeF_2 interface, and then perpendicular to the applied field in the FeF_2 bulk (ϕ_{FeF2}= -89±5°).[34] The tendency for the Co magnetization and the net uncompensated magnetization in the FeF_2 to rotate in opposition is evident in the change of sign of the component of the magnetization perpendicular to the applied field $M_{\perp} = M(z)\sin(\phi(z))$ (dashed-black curve, Figure 4).[35] The twist of the magnetization across the Co/FeF_2 interface is reminiscent of a domain wall parallel to the interface between soft and hard magnetic materials, as found for example in exchange spring magnets[36,37] or in the computational model proposed by Kiwi *et al.* [38] to explain exchange bias in Fe/FeF_2 bilayers. The rotation of the uncompensated magnetization close to the Co/FeF_2 interface provides a natural explanation for the experimental observation that an antiferromagnet must exceed a critical thickness, t_c (Figure 1), before bias is produced.[39]

In a previous study of the influence of crystalline quality of FeF_2 films on exchange bias,[40] exchange bias was found to be small for single crystal FeF_2 films grown on FeF_2 bulk single crystals—a recipe that minimizes misfit strain in the thin film lattice—in contrast to the substrate (MgF_2) used to make the sample reported presently. The accommodation of misfit strain through the formation of defects may be an important factor affecting the antiferromagnetic domain state and exchange bias. We note that previously large exchange bias in Co/$Co_xO_{(1-x)}$ bilayers was attributed to uncompensated magnetization in the bulk of non-stoichometric CoO antiferromagnet.

We used the micromagnetic simulation package OOMMF[41] to determine whether the magnetization profile deduced from neutron scattering was consistent with a low energy magnetic configuration for the conditions of our experiment. We treated the interface and uncompensated spins in the FeF_2 layers as if they were slightly ferromagnetic, and assigned saturation magnetizations of 1212, 400 and 67 kA/m to the Co, interface and FeF_2 layers, respectively, to mimic the magnetization profile in Figure 4 (●). Values for the exchange stiffness of $30x10^{-12}$ and $1.23x10^{-12}$ J/m were used for Co and FeF_2, respectively, and the average of these values assigned to the interface layer. Values for the uniaxial anisotropy of

4.5x10^{5} and 1.76x10^{6} J/m^{3} were used for Co and FeF_2, respectively. We included two adjustable parameters in the simulation—the interface exchange constant J_{int} across the Co-interface layers and the anisotropy of the interface K_{int}. Values of J_{int} = -1.5 x10^{-3} to -2.0x10^{-3} J/m^{2} and K_{int} = 1x10^{5} J/m^{3} yield the direction of the vector magnetization in Figure 4 (■), in good agreement with the neutron scattering result. The micromagnetic simulation was repeated using the same magnetic model, but with the field applied along [001] FeF_2 and varied between ±477 kA/m. With the initial configuration of all three layers aligned in the positive direction, which is equivalent to cooling the sample in a large magnetic field, this simulation yielded a positively shifted hysteresis loop. This confirms that due to large anisotropy, the moments in the bulk FeF_2 remain pinned in the initial direction.

In conclusion, we have performed experiments that actively perturbed the magnetic structure of a Co/FeF_2 system—one exhibiting large exchange bias—in order to measure the depth profiles of the pinned and unpinned magnetization. For a system with +167 kA/m exchange bias, we found that the antiferromagnetic FeF_2 layer possesses uncompensated magnetization. The uncompensated FeF_2 magnetization is anti-parallel to the Co spins across the Co/FeF_2 interface, and the net uncompensated magnetization within 2 to 3.5 nm of this interface rotates in conjunction with the Co spins. However, at distances greater than ~3.5 nm from the interface, the uncompensated FeF_2 magnetization is pinned providing a means to establish bias. Micromagnetic simulation confirms the magnetization depth profile deduced from neutron reflectometry is a low energy configuration, and the model structure yields a positively shifted hysteresis loop.

The facilities of the Manuel Lujan Jr. Neutron Scattering Center and the Advanced Light Source are gratefully appreciated. Discussions with M.J. Donahue, D. Lederman, K.

Liu and R.D. McMichael are gratefully acknowledged. This work was supported in part by the Office of Basic Energy Science, U.S. Department of Energy, BES-DMS, the University of California Campus Laboratory Collaborative program, and Laboratory Directed Research and Development program funds. Also, financial support from the Alexander-von-Humboldt Foundation (O.P.), Cal(IT)^2 (Z.-P. L.), Spanish MECD (R.M. and X.B.), Fulbright Commission (R.M.), Catalan Dursi (X.B.), and the Swiss National Science Foundation (M.D.) is acknowledged.

Figure 1 Element specific hysteresis loops at Q = 0.49 and 0.38 nm^{-1} for Co (■) and Fe (●), respectively. Inset: The geometry of the X-ray experiment and a representation of the sample are shown (layers spaced apart for the sake of clarity).

Figure 2 Relative variation of the spin density profile for Co and Fe spins with the magnetic field applied parallel (and anti-parallel) to [001] FeF_2 obtained from the specular reflectivity shown in the inset for Fe and Co (shifted by a factor of 10^{-2} for the sake of clarity) for fixed incident beam polarization.

Figure 3 Polarized neutron reflectivity (symbols) of the exchange-biased sample at 10 K with H = 438 kA/m along $[\bar{1}10]$ FeF_2. These data comprising 300 experimental points required approximately seven days to acquire. The solid curves are the reflectivities calculated from a model whose magnetization depth profile is shown in **Figure 4**. Inset: Unpinned magnetization follows the applied field and produces splitting of the non-spin-flip (R^{++} and R^{--}) reflectivities. Magnetization with a component along [001] FeF_2 produces spin-flip scattering, R^{SF}.

Figure 4 Depth dependence of the vector magnetization (3D-view,inset) magnitude (blue curve, $|\vec{M}|$) and angular deviation, ϕ, from the applied field in the sample plane (red curve) deduced from the neutron reflectivity data (**Figure 3**). The magnetization used in the OOMMF simulation (●) and the values of ϕ (■) obtained from the simulation. The projection of the sample magnetization along the incident soft X-ray beam (corresponding to the conditions of the soft X-ray experiment) is shown as (○) in absolute units. Error bars represent the deviation of the corresponding profiles whose figures of merit were indistinguishable.

Figure 1

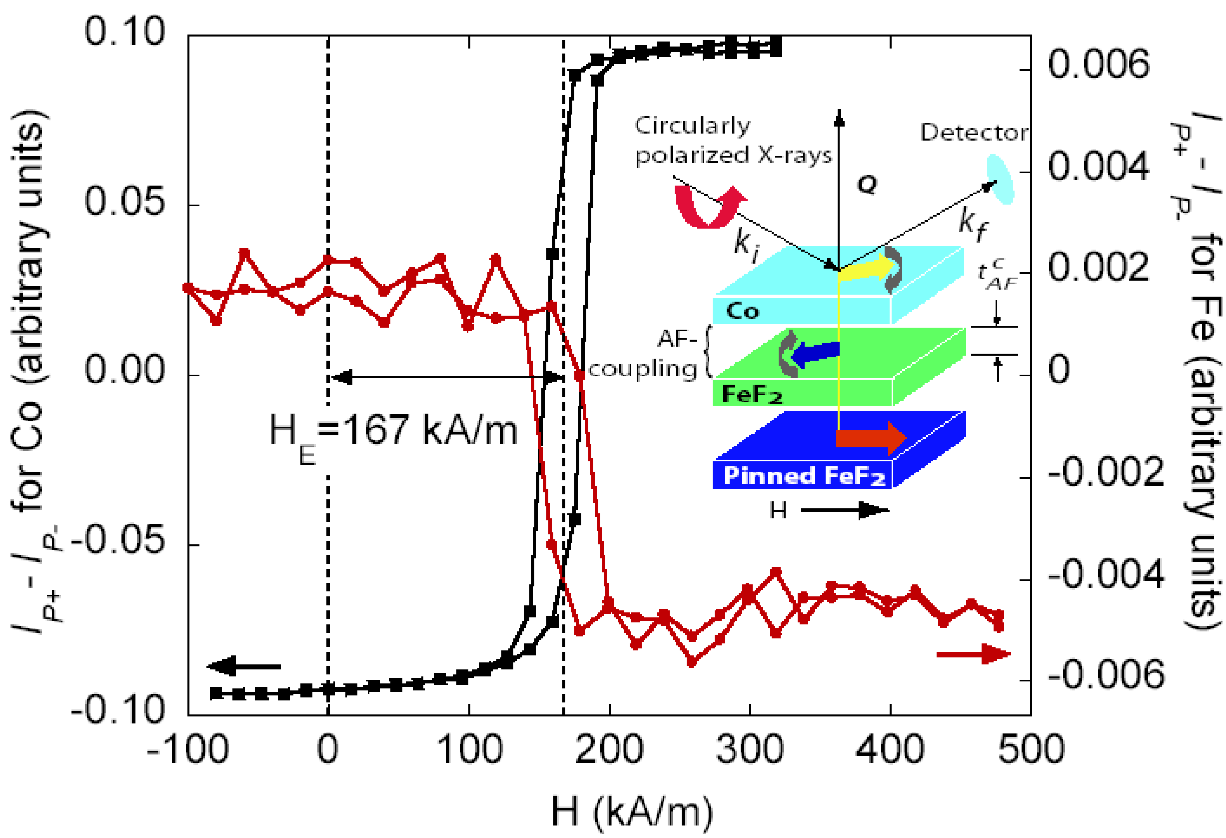

0.10
0.05
0.00
-0.05
-0.10
-100
0
100
200
300
400
500
H (kA/m)
$I_{P+} - I_{P-}$ for Co (arbitrary units)
0.006
0.004
0.002
0
-0.002
-0.004
-0.006
$I_{P+} - I_{P-}$ for Fe (arbitrary units)
H_E=167 kA/m
Circularly
polarized X-rays
Detector
Q
k_i
k_f
t^c_{AF}
Co
AF-
coupling
FeF2
Pinned FeF2
H

Figure 2

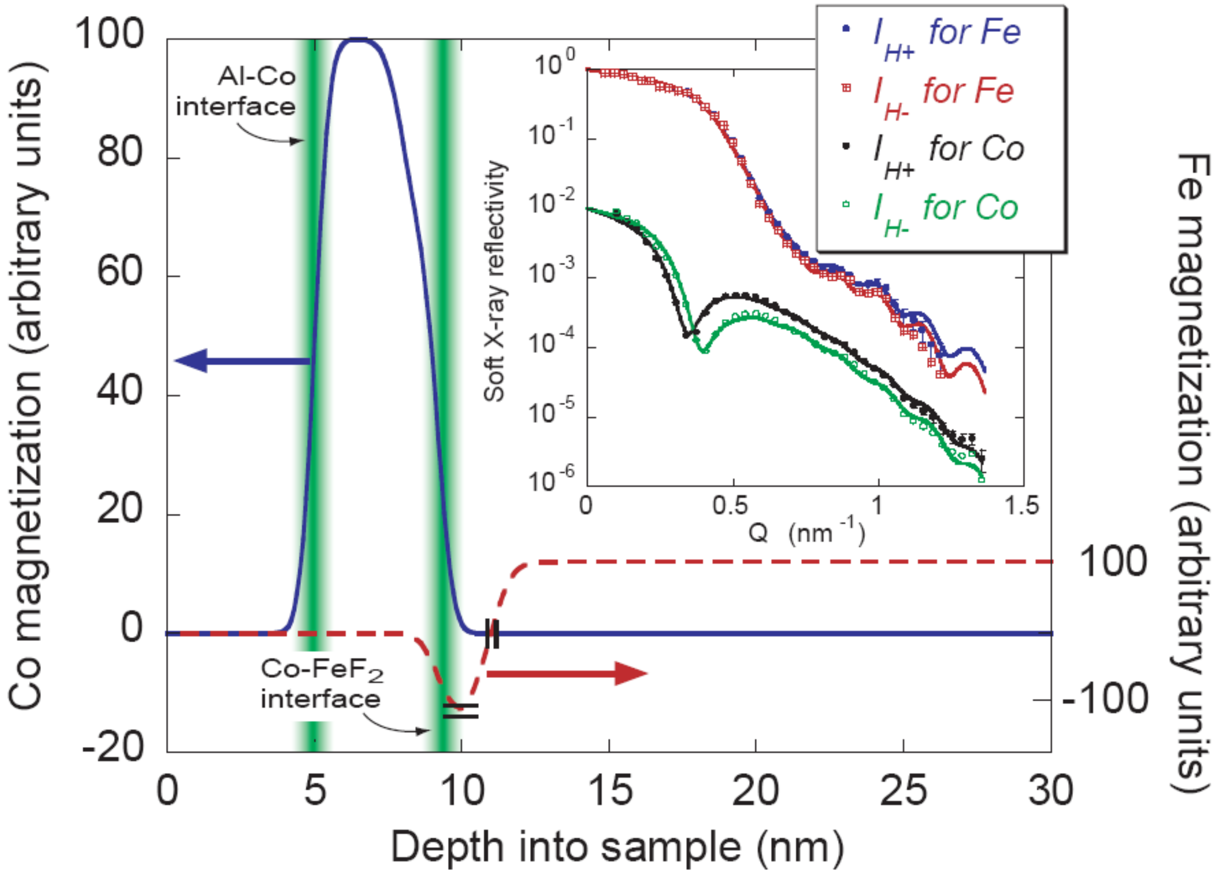

Al-Co
interface
Co-FeF2
interface
Co magnetization (arbitrary units)
Fe magnetization (arbitrary units)
Depth into sample (nm)
Soft X-ray reflectivity
Q (nm -1)
I H+ for Fe
I H- for Fe
I H+ for Co
I H- for Co

Figure 3

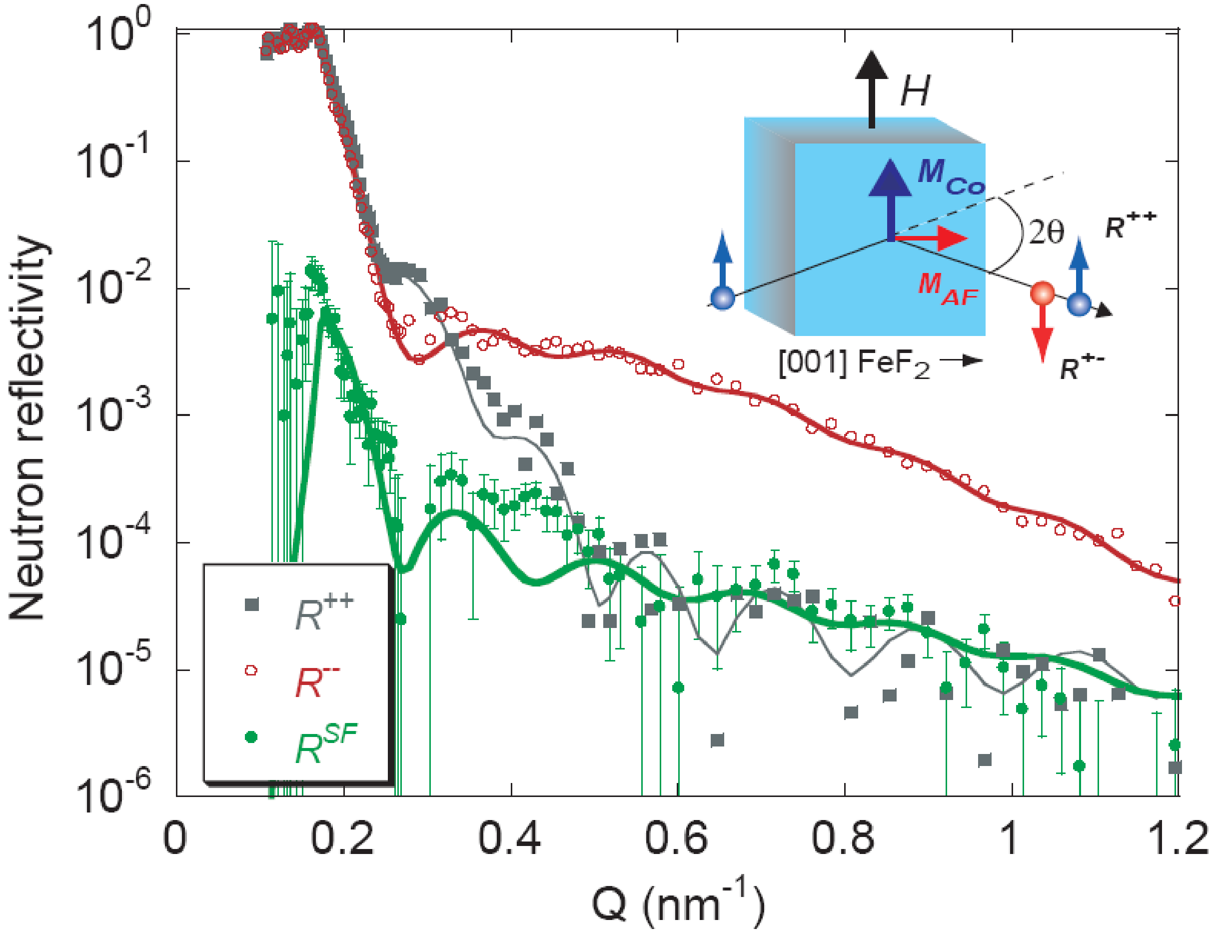

H
M_{Co}
2θ
R^{++}
M_{AF}
[001] FeF$_2$
R^{+-}
R^{++}
R^{--}
R^{SF}
Neutron reflectivity
10^0
10^{-1}
10^{-2}
10^{-3}
10^{-4}
10^{-5}
10^{-6}
0
0.2
0.4
0.6
0.8
1
1.2
Q (nm^{-1})

Figure 4

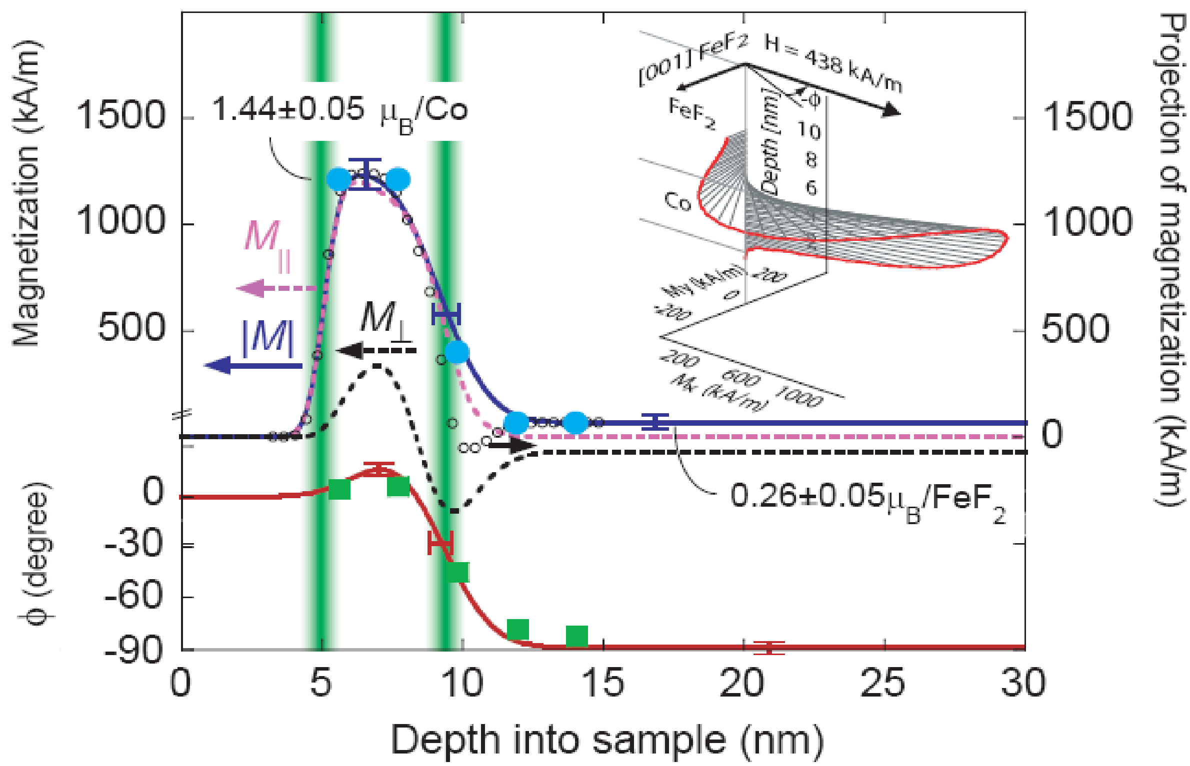

Magnetization (kA/m)
Projection of magnetization (kA/m)
φ (degree)
1.44±0.05 μB/Co
0.26±0.05μB/FeF2
M||
M⊥
|M|
[001] FeF2
H = 438 kA/m
FeF2
Co
Depth [nm]
My [kA/m]
Mx (kA/m)
Depth into sample (nm)

References

1 M.R. Fitzsimmons *et al.*, *J. Magn. Magn. Mater.* **271**, 103 (2004).

2 W.H. Meiklejohn, C.P. Bean, *Phys. Rev.* **105**, 904 (1957).

3 J. Nogués, I.K. Schuller, *J. Magn. Magn. Mater.* **192**, 203 (1999).

4 A.E. Berkowitz, K. Takano, *J. Magn. Magn. Mater.* **200**, 552 (1999).

5 R.L. Stamps, *J. Phys. D: Appl. Phys.* **33**, R247 (2000).

6 M. Kiwi, *J. Magn. Magn. Mater.* **234**, 584 (2001).

7 M.R. Fitzsimmons *et al.*, *Phys. Rev. Lett.* **84**, 3986 (2000).

8 I.N. Krivorotov, C. Leighton, J. Nogués, I.K. Schuller, E.D. Dahlberg, *Phys. Rev. B* **68**, 54430 (2003).

9 A. Hoffmann, *Phys. Rev. Lett.* **93**, 097203 (2004).

10 H. Shi *et al., J. Appl. Phys.* **93**, 8600 (2003).

11 Ch. Binek, Xi Chen, A. Hochstrat, W. Kleemann, *J. Magn. Magn. Mater.* **240**, 257 (2002).

12 P. Miltényi *et al.*, Phys. Rev. Lett., **84**, 4224 (2000).

13 Hongtao Shi *et al., J. Appl. Phys.*, **93**, 8600 (2003).

14 A. Hoffmann *et al., Phys. Rev. B* **66**, 220406(R) (2002).

15 H. Ohldag *et al., Phys. Rev. Lett.* **91**, 017203 (2003).

16 The three-dimensional net magnetization vector can be obtained with polarized neutron scattering; however, in our application, i.e., polarized neutron reflectometry, only the projection of the three-dimensional net magnetization vector onto the sample plane is obtained.

17 S.A. Stepanov, S.K. Sinha, *Phys. Rev. B* **61**, 15302 (2000).

18 D.R. Lee *et al., Phys. Rev. B* **68**, 224409 (2003).

19 R.M. Osgood III, S.K. Sinha, J.W. Freeland, Y.U. YIdzerda, S.D. Bader, *J. Magn. Magn. Mater.* **198-199**, 698 (1999).

20 S. Park, M.R. Fitzsimmons, X.Y. Dong, B.D. Schultz, C.J. Palmstrøm, *Phys. Rev. B* **70**, 104406 (2004).

21 The (110) plane of FeF_2 in bulk single crystals has no net magnetic moment (i.e. is compensated).

22 D.B. Williams, C.B. Carter, *Transmission Electron Microscopy* (Plenum press, NY 1996), p. 447.

23 L.B. Freund, *MRS Bulletin* **17**, 52 (1992).

24 Since the L_3 edges of Co and Fe occur at different X-ray wavelengths, measurements taken at the same angles of incidence and reflection (such as ours) will correspond to slightly different wave vector transfers.

25 In principle, the vertical shift of the Fe hysteresis loop might indicate the presence and direction of pinned spins relative to the cooling field. However, we found that in switching the polarization of the X-ray beam (accomplished by moving the undulator at the synchrotron source), the vertical shift of the Fe hysteresis loop would change magnitude and sign, even when all other instrument variables were left unchanged. Therefore, we conclude the vertical shift of the hysteresis loop is an instrumental artifact. We note, the horizontal shift of the loops (the exchange bias), coercivity and relationship of the Fe loop to the Co loop (i.e., inverted) were always reproducible.

26 P.R. Bevington, D.K. Robinson, *Data Reduction and Error Analysis for the Physical Sciences*, (McGraw Hill, Boston, MA, ed. 3, 2003) p. 67.

27 Measurements of magnetization obtained with polarized soft X-ray beams are usually not obtained in absolute units (we used neutron scattering to establish an absolute scale for the X-ray results).

28 G.P. Felcher *et al.*, *Rev. Sci. Instrum.* **58**, 609 (1987).

29 C.F. Majkrzak, *Physica B* **221**, 342 (1996).

30 Since the magnetization vector obtained from specular neutron reflectometry is the projection of the net magnetization vector onto the sample's surface, we are not able to discern a canting of the sample magnetization out of the sample plane.

31 L.G. Parratt, *Phys. Rev.* **95**, 359 (1954).

32 The magnitude of the Co magnetization, M_{Co}, was obtained from neutron data collected when the sample temperature was 108 K.

33 The magnetic widths of the Co/interface and interface/FeF_2 were determined to be 1.5±0.1 nm.

34 The neutron scattering data are sensitive to the orientation of the FeF_2 magnetization relative to the Co magnetization. The key point is that our data indicate the magnetizations in the two layers move in opposite directions.

35 The tendency for the Co magnetization to oppose the rotation of the FeF_2 magnetization near the Co/FeF_2 interface is not contrived. The starting configuration was one that began with a twist of the same sign

across the interface, and yet, evolved towards a situation in which the Co magnetization tended to rotate in a direction that opposed the rotation of the FeF_2 magnetization.

36 O. Hellwig, J.B. Kortright, K. Takano, E.E. Fullerton, *Phys. Rev. B* **62**, 11694 (2000).

37 K.V. O'Donovan, J.A. Borchers, C.F. Majkrzak, O. Hellwig, E.E. Fullerton, *Phys. Rev. Lett.* **88**, 067201 (2002).

38 M. Kiwi, J. Mejía-López, R.D. Portugal, R. Ramírez, *Appl. Phys. Lett.* **75**, 3995 (1999).

39 M.S. Lund *et al.*, *Phys. Rev. B* **66**, 054422/1-7 (2002).

40 M.R. Fitzsimmons *et al.*, *Phys. Rev. B*, **65**, 134436 (2002).

41 M.J. Donahue and D.G. Porter, “OOMMF User’s Guide Version 1.0,” NISTIR 6376, National Institute of Standards and Technology, Gaithersburg, MD (1999).